



**Copper transporters and chaperones CTR1, CTR2, ATOX1,
and CCS as determinants of cisplatin sensitivity**

Journal:	<i>Metallomics</i>
Manuscript ID	MT-ART-03-2016-000076.R1
Article Type:	Paper
Date Submitted by the Author:	26-Apr-2016
Complete List of Authors:	Bompiani, Kristin; University of California San Diego, Moores Cancer Center Tsai, Cheng-Yu; University of California, San Diego, Moores Cancer Center Achatz, Felix; University Medical Centre Regensburg Liebig, Janika; Friedrich-Alexander-University Erlangen-Nurnberg, Institute of Biochemistry, Emil-Fischer-Zentrum Howell, Stephen; University of California, San Diego, Medicine

1
2
3 **Copper transporters and chaperones CTR1, CTR2, ATOX1, and CCS as**
4
5
6 **determinants of cisplatin sensitivity**
7
8
9

10
11 Kristin M. Bompiani^a, Cheng-Yu Tsai^a, Felix P. Achatz^b, Janika K. Liebig^c, and Stephen B.
12
13 Howell^{a*}
14
15
16
17
18
19

20
21 ^a Moores Cancer Center, University of California, San Diego; 3855 Health Sciences Drive, Mail
22
23 Code 0819, La Jolla, CA 92093
24

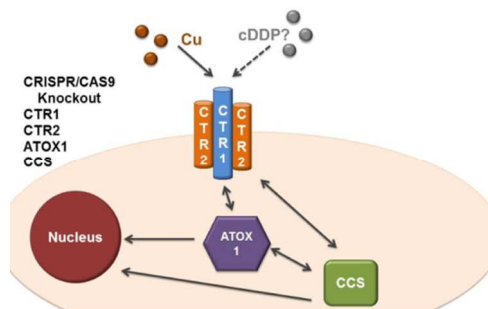
25 ^b University Medical Centre Regensburg, Regensburg, Germany
26

27
28 ^c Institute of Biochemistry, Emil-Fischer-Zentrum, Friedrich-Alexander-University Erlangen-
29
30 Nürnberg, Erlangen, Germany
31
32
33
34
35
36
37
38

39
40 *To whom correspondence should be addressed: Stephen B. Howell, MD, Moores UCSD Cancer
41
42 Center, 3855 Health Sciences Drive, Mail Code 0819, La Jolla, CA 92093-0819, USA; Tel. 1-
43
44 (858) 822-1110; Fax 1-(858) 822-1111; email: showell@ucsd.edu
45
46
47
48
49
50
51
52
53
54
55
56
57
58
59
60

Table of contents entry

We used CRISPR-Cas9 technology to address whether copper transporters or chaperones CTR1, CTR2, ATOX1, and CCS mediate cisplatin sensitivity in human cells.



Abstract

The development of resistance to cisplatin (cDDP) is commonly accompanied by reduced drug uptake or increased efflux. Previous studies in yeast and murine embryonic fibroblasts have reported that the copper (Cu) transporters and chaperones participate in the uptake, efflux, and intracellular distribution of cDDP. However, there is conflicting data from studies in human cells. We used CRISPR-Cas9 genome editing to individually knock out the human copper transporters CTR1 and CTR2 and the copper chaperones ATOX1 and CCS. Isogenic knockout cell lines were generated in both human HEK-293T and ovarian carcinoma OVCAR8 cells. All knockout cell lines had slowed growth compared to parental cells, small changes in basal Cu levels, and varying sensitivities to Cu depending on the gene targeted. However, all of the knockouts demonstrated only modest 2 to 5-fold changes in cDDP sensitivity that did not differ from the range of sensitivities of 10 wild type clones grown from the same parental cell population. We conclude that, under basal conditions, loss of CTR1, CTR2, ATOX1, or CCS does not produce a change in cisplatin sensitivity that exceeds the variance found within the parental population, suggesting that they are not essential to the mechanism by which cDDP enters these cell lines and is transported to the nucleus.

Keywords: ATOX1, cisplatin, CCS, copper, CRISPR, CTR1, CTR2

Significance to Metalloomics

Prior studies have suggested a role for Cu homeostasis proteins in the cellular pharmacology of the platinum-containing drugs. However, using the more definitive approach of CRISPR-Cas9-mediated gene knockout this study shows that neither the loss of Cu transport proteins (CTR1 or

1
2
3 CTR2), nor the knockout of two Cu chaperones (ATOX1 and CCS), modulated sensitivity to the
4
5
6 chemotherapeutic agent cisplatin in two different types of neoplastic cell lines.
7
8
9
10
11
12
13
14
15
16
17
18
19
20
21
22
23
24
25
26
27
28
29
30
31
32
33
34
35
36
37
38
39
40
41
42
43
44
45
46
47
48
49
50
51
52
53
54
55
56
57
58
59
60

Introduction

Cisplatin (cDDP) is an important chemotherapeutic agent that is an essential member of treatment programs for many types of cancer. Although initially effective, many tumors gradually become resistant during therapy with cDDP, and resistance is often accompanied by reduced drug uptake. cDDP is highly polar and its ability to diffuse across plasma membranes is thought to be limited, suggesting the presence of a transport system. Previous studies have suggested a role for copper (Cu) transporters in the uptake and efflux of cDDP ¹.

Copper is essential to the growth of eukaryotic cells but can also be toxic due to its ability to undergo redox reactions that generate oxygen free radicals. A complex system of transporters and chaperones has evolved to manage Cu homeostasis. The Cu proteome is well conserved from yeast to humans with many of the proteins sharing conserved motifs that bind Cu. Cu is imported into the cell predominantly through the high-affinity transporter CTR1, which is a surface membrane-bound receptor that forms a homotrimer ^{2,3}. Structural models predict that the extracellular domain of CTR1 forms a pore that directly imports Cu ⁴. Increasing the extracellular concentration of Cu causes CTR1 internalization, which limits additional Cu import and potential toxicity ⁵. A second Cu transporter, CTR2, has also been identified, although its role in Cu homeostasis is less clear. CTR2 has been proposed to form a heterotrimer with CTR1 on the cell surface to support pore formation ⁶, and is additionally localized to endosomes and lysosomes ⁷. Yeast CTR2 has been shown to regulate internal pools of Cu under low Cu conditions ^{8,9}, suggesting that the human homolog may have a similar Cu regulatory function. Recent studies found that CTR2 plays a role in mast cell maturation and hemostasis ¹⁰, and that CTR1 protects CTR2 protein from degradation ¹¹.

1
2
3
4
5
6
7
8
9
10
11
12
13
14
15
16
17
18
19
20
21
22
23
24
25
26
27
28
29
30
31
32
33
Once inside the cell, the concentration and location of Cu is tightly controlled as it is shuttled throughout subcellular compartments via interactions with Cu chaperones. The human copper chaperone for superoxide dismutase 1 (CCS) directly donates Cu to the enzyme SOD1 to support antioxidant activity^{12, 13}. Antioxidant 1 (ATOX1) donates Cu to the efflux Golgi-associated transporters ATP7A and ATP7B, which incorporate Cu into proteins, such as ceruloplasmin and lysyl oxidase, or into vesicles for secretion or export of excess Cu when levels are elevated^{14, 15}. Recent reports have also shown that Cu-laden ATOX1 migrates to the nucleus and may have transcription-factor like activity that supports cell growth¹⁶. Whether ATOX1 and CCS directly acquire Cu from CTR1 or CTR2 or another intermediate Cu chaperone is unclear, although the two chaperones have been shown to directly interact and transfer Cu¹⁷. Data recently published by Wang *et al.* show that ATOX1 or CCS knockdown decreases cell proliferation and tumor growth by modulating ATP levels and lipogenesis, and that an ATOX1/CCS targeting small molecule has similar effects¹⁸.

34
35
36
37
38
39
40
41
42
43
44
45
46
47
48
49
50
51
52
53
54
55
56
57
58
59
60
Data from several labs has suggested that proteins within the Cu homeostasis pathway mediate uptake and efflux of cDDP. CTR1 gene deletion in yeast and mouse embryonic fibroblasts (MEFs) decreased cDDP uptake and increased resistance, suggesting it may be the primary transporter for drug influx^{19, 20}. CTR1 mRNA and protein expression levels correlate with cDDP response and post-treatment survival²¹⁻²³. In contrast to CTR1, the role of CTR2 in platinum drug cellular pharmacology is less well characterized. Expression levels correlate with treatment success in patients^{24, 25} and cDDP sensitivity²⁶, and CTR2 knockdown or knockout cells have increased levels of cDDP uptake^{6, 27}. cDDP also binds the Cu chaperone COX17 in solution, and COX17 mediates mitochondrial delivery which, in turn, affects cDDP sensitivity through non-DNA related apoptosis pathways²⁸. cDDP has also been shown to bind ATOX1 in

1
2
3 solution ^{29,30} and in cells ³¹. ATOX1 knockout mutations in both *Drosophila* and MEFs
4
5 engendered resistance to cDDP ^{32,33}. Consequentially, ATOX1 was hypothesized to bind and
6
7 transport cDDP to the nucleus. ATOX1 may also play a role in cDDP detoxification through
8
9 transfer to ATP7A or ATP7B. ATP7A and ATP7B protein levels were reported to be
10
11 upregulated in cDDP resistant ovarian ^{34,35} and oral squamous cell carcinoma cell lines ³⁶.
12
13 ATP7B overexpression in epidermoid carcinoma KB-3-1 cells also engendered cDDP resistance
14
15 ³⁷. Although no data has been reported for the direct interaction of CCS with cDDP, ATOX1,
16
17 CCS and the transporters ATP7A and ATP7B share a conserved CXXC Cu chelating motif that
18
19 coordinated cDDP in the crystal structure of ATOX1 ²⁹ and the soluble first domain of ATP7A
20
21 ³⁸. Despite all of these studies, there remains controversy as to the ability of the Cu homeostasis
22
23 system to participate in the transport of cDDP or modulate sensitivity to this important drug ^{39,40}.
24
25
26
27
28

29 We used CRISPR-Cas9 genome editing to individually knockout CTR1, CTR2, ATOX1,
30
31 and CCS in neoplastic human HEK-293T and ovarian cancer OVCAR8 cells. We report here
32
33 that knockout of CTR1, CTR2, ATOX1, and CCS produced only a modest change in sensitivity
34
35 to cDDP. These isogenic knockout cell lines targeting multiple steps within the same pathway
36
37 provide compelling evidence that these Cu transporters and chaperones are not the primary
38
39 uptake and transport mechanism for cDDP in these cell lines.
40
41
42
43
44
45

46 **Methods**

47 **Cell culture and reagents**

48
49 Human Embryonic Kidney 293T (HEK-293T) cells were obtained from ATCC (Manassas, VA).
50
51 The wild type 293T and all sublines were cultured in DMEM medium (HyClone, Logan, UT)
52
53 supplemented with 10% fetal bovine serum (Lonza, Basel, Switzerland), 1 mM sodium pyruvate
54
55
56
57
58
59
60

1
2
3 (Lonza, Basel, Switzerland), 2 mM glutamine (Thermo Scientific, Waltham, MA) and 1X
4 penicillin/streptomycin (Corning Life Sciences, Corning, NY). Ovarian Carcinoma 8 (OVCAR8)
5
6 cells were received from Dr. Tom Hamilton, Fox Chase Cancer Center (Philadelphia, PA). All
7
8 OVCAR8 cell lines were cultured in RPMI 1640 medium (HyClone) supplemented with 10%
9
10 FBS and 1X penicillin/streptomycin. Both cell lines were grown at 37°C with 5% CO₂ and tested
11
12 negative for mycoplasma contaminated with a MycoSensor PCR kit (Agilent, Santa Clara, CA).
13
14
15
16

17 **CRISPR-Cas9 genome engineering and knockout screening**

18
19 Generation of the CTR1 and CTR2 knockout clones has been previously described¹¹. For
20
21 ATOX1 and CCS knockout, single guide RNA (sgRNA) design and delivery was performed as
22
23 previously described⁴¹. The online CRISPR design tool (<http://crispr.mit.edu/>) was used to
24
25 design guide RNAs targeting ATOX1 exon 2 on the coding strand and CCS exon 1 on the coding
26
27 strand. Complementary guide oligonucleotides (ATOX1 5'-
28
29 TCTCGGGTCCTCAATAAGCTTGG-3; CCS 5'- CACCGCTTCGGATTCGGGGAACCA-3')
30
31 were custom synthesized by Integrated DNA Technologies (Coralville) and ligated into
32
33 pSpCas9(BB)-2A-GFP (pX458) (Addgene, Cambridge, MA). CRISPR plasmids were transiently
34
35 transfected into HEK-293T or OVCAR8 cells with Lipofectamine 2000 (Life Technologies, Inc.,
36
37 Grand Island, NY). The transfected population was FACS sorted for GFP expression 48 h after
38
39 transfection. Single cells were sorted into 96 well plates and grown into populations over a
40
41 period of 3 weeks. Populations were expanded, and DNA was harvested from confluent 12-well
42
43 plates with a QIAmp DNA mini kit (Qiagen, Valencia, CA). Genomic DNA was amplified with
44
45 ATOX1 primers (F 5'-TCCTGCCCAGTC TCTCTGTCTT-3'; R:5'-
46
47 CCATGGCTCCAGAGCTACTCCT-3') or CCS primers (F 5'-
48
49 GGGTTACTAAGGCAACCAGGA-3'; R 5'- GAGGCTTCTGGACTGTCTGC -3') spanning
50
51
52
53
54
55
56
57
58
59
60

1
2
3 the target cut site. Amplicons were digested with BamHI and HindIII (New England Biolabs,
4 Ipswich, MA), ligated into pUC19 (Invitrogen, Grand Island, NY), and transformed into
5 DH5alpha bacteria (Invitrogen) using standard molecular biology techniques. A minimum of 10
6 bacterial clones were sequenced per each knockout cell line.
7
8
9
10
11

12 **Western blotting**

13
14
15 Cells were washed with ice cold PBS, then lysed in ice-cold RIPA buffer (50 mM Tris-HCl pH
16 8.0; 150 mM NaCl; 1 mM EDTA, 1% Triton X-100; 0.1% SDS; 0.5% sodium deoxycholate)
17 supplemented with 1X Halt protease inhibitor cocktail (Thermo Fisher Scientific). Protein
18 contents of the lysates were determined with the *DC*-Protein assay kit (Bio-Rad; Hercules, CA).
19
20 Fifty micrograms of total protein was boiled with Laemmli dye for 5-10 minutes, then loaded on
21 Tris-Glycine or Tris-Tricine gels and electrotransferred to low fluorescence PVDF membranes
22 (EMD Millipore, Billerica, MA). Blots were stained with 1:1000 anti-CTR1 (gift from Dr.
23 Marcus Kuo⁴²), 1:1000 mouse anti-CTR2 (National Cancer Institute⁴³), 1:1000 rabbit anti-
24 ATOX1 (Abcam, Cambridge, MA) or 1:1000 rabbit anti-CCS (Santa Cruz Biotechnology, Dallas,
25 TX) and 1:1000 mouse β -actin (Cell Signaling Technologies, Danvers, MA) primary antibodies
26 overnight at 4°C. The blots were counter stained with 1:10,000 goat-anti rabbit 680LT and
27 1:5,000 goat-anti-mouse-800CW secondary antibodies (Li-Cor Biosciences, Lincoln, NE) and
28 imaged with a Li-Cor Odyssey Imager (Li-Cor Biosciences). Images were quantified with *Image*
29 *J* software (NIH, <http://imagej.nih.gov/ij/>).
30
31
32
33
34
35
36
37
38
39
40
41
42
43
44
45
46
47

48 **cDDP cytotoxicity assay**

49
50 Cells were plated in sextuplicate in 96-well plates at a density of 3,000 cells/well. The cells were
51 incubated for 16-24 hours and then treated with increasing doses of cisplatin (0-100 μ M; Teva
52 Parenteral Medicines, Inc., Irvine, CA) for 1 hour. After 1 hour, the cDDP media was aspirated
53
54
55
56
57
58
59
60

1
2
3 and replaced with fresh media. The plates were incubated for an additional 96 hours, and the cell
4
5 viability was determined with CCK-8 assay kit (Clonetech, Inc., Mountain View, CA). Five
6
7 microliters of CCK-8 reagent was added per well, the plates were incubated at 37°C for 4 hours,
8
9 and absorbance was read at 450 nm with an Molecular Devices microplate reader (Sunnyvale,
10
11 CA).

12 13 14 **Copper sensitivity assay**

15
16 Cells were plated in quadruplicate in 96-well plates at a density of 3,000 cells/well. The cells
17
18 were incubated for 16-24 hours and then treated with increasing doses of CuSO₄ continuously for
19
20 96 hours. Cell viability was determined with CCK-8 assay kit (Clonetech, Inc., Mountain View,
21
22 CA) as described above. The data were fit with a linear trend line to calculate and compare Cu
23
24 sensitivity.
25
26

27 28 29 **Cell growth curve assay**

30
31 Cells were plated in quadruplicate in 96-well plates at a density of 2,000 cells/well. The cells
32
33 were incubated for 1-7 days, and the cell viability was quantified every 24 hours with CCK-8
34
35 reagent as above. Cell growth was log₁₀ transformed and graphed over time. The linear portion
36
37 of the data was fit with a linear regression to calculate and compare cell growth rates.
38
39

40 41 42 **Basal copper levels (ICP-MS)**

43
44 HEK-293T cells were plated at a cell density of 0.5x10⁶ (wildtype) – 0.75*10⁶ cells (KOs) in
45
46 two 6-well plates per cell line and incubated for 48-72 hours until 80-90% confluent. One 6 well
47
48 plate was used to measure protein concentrations and the second was for Cu. The protein control
49
50 plate was washed once with ice-cold PBS then lysed with 100 uL of ice-cold RIPA-Buffer
51
52 supplemented with 1X Halt protease Inhibitor cocktail. Protein samples were stored at -80°C and
53
54 the protein concentration was quantified with a BD BioRad protein quantification kit. The
55
56
57
58
59
60

1
2
3 protein concentration was averaged for the 6 repeat wells. For the Cu samples, the cells were
4
5 washed with ice-cold Cu-free PBS three times. Cell pellets were dissolved in 215 uL of 70%
6
7 nitric acid at room temperature overnight, then diluted the next morning in 6 mL of ICP-MS
8
9 buffer (0.1% Triton X, 1% Nitric acid, 1 ppb Indium, diluted in Cu-free water). ⁶⁴Cu levels were
10
11 measured with an iCAP inductively coupled plasma mass spectrometer at the Scripps Institute of
12
13 Oceanography (Thermo Scientific, Waltham, MA). Cu concentrations were normalized to the
14
15 average protein concentration for that cell line.
16
17
18

19 **Nude mice xenografts**

20
21 All animal work was approved by the UCSD Institutional Animal Care and Use Committee
22
23 (IACUC). Female BALB/c nu/nu mice 6-8 weeks old were injected subcutaneously with 1×10^6
24
25 cells (150 uL) diluted 1:1 in PBS:Matrigel (BD Biosciences, Franklin Lakes, NJ). Mice were
26
27 injected bilaterally at the left and right shoulder and flank regions (4 inoculation sites per mouse,
28
29 2-4 mice per group, n=8 to 16 injections per cell line). Once palpable, tumor volume was
30
31 recorded twice per week, log₁₀ transformed and graphed over time. Linear regression was used
32
33 to calculate and compare the tumor growth rates.
34
35
36
37

38 **Statistical analyses**

39
40 Data presented represent the mean \pm SEM of at least three independent experiments performed in
41
42 at least triplicates. Student's t-test p-values of the individual KOs compared to WT were
43
44 calculated with GraphPad Prism (GraphPad, La Jolla, CA), and P-values < 0.05 were considered
45
46 significant.
47
48
49
50

51 **Results**

Knockout cell line generation with CRISPR-Cas9 genome editing

The bacterial CRISPR-Cas9 system was used to generate human isogenic knockout cell lines that completely lack detectable levels of the target protein. The CTR1, CTR2, ATOX1, and CCS genes were independently edited using the CRISPR-Cas9 technique and the tools initially described by the Zhang laboratory⁴¹. Generation of the CTR1 and CTR2 knockouts was previously described¹¹. Guide RNAs were designed with the online CRISPR design tool (<http://crispr.mit.edu/>) and cloned into the pSpCas9(BB)-2A-GFP (pX458) vector. Exon 2 was targeted in CTR1, exon 3 in CTR2, exon 2 in ATOX1, and exon 1 in CCS. We edited each gene in two different human cell lines, the neoplastic HEK-293T cell line and the OVCAR8 human ovarian carcinoma line. Parental cell populations were transiently transfected with the appropriate vector, and GFP-positive single cells were sorted by FACS into individual wells 48 h after transfection. For each gene targeted genes, approximately 50 single cell clones were expanded into populations over the course of 3 weeks. PCR primers flanking the targeted editing site were designed to generate an amplicon, and sequencing of the expanded populations indicated numerous clones (>40%) had mutations in the individual target genes. Candidate mutant clones were further screened by Western blotting with whole cell lysates to assess target protein expression. Multiple clones that lacked protein expression were identified for each gene indicating that CRISPR-Cas9 targeting and knockout was successful. Two clones per gene (KO1 and KO2) for each cell type were further characterized using standard molecular cloning techniques to sequence the individual alleles. Sequencing indicated that the KO clones contained small insertions or deletions near the targeted CRISPR cut site on both alleles (Table 1). All of the DNA in/dels in the 2 clones selected for each gene were predicted to cause a frameshift mutation and introduce an early downstream stop codon on both alleles resulting in a severely

1
2
3 truncated, out of frame, or unstable protein (Table 2). A total of 16 clonal cell lines were
4
5 generated for comparison: two knockout clones per gene (CTR1, CTR2, ATOX1, and CCS) in
6
7 each of two cell lines (HEK-293T and OVCAR8). Figure 1 shows Western blot analyses of each
8
9 KO cell line confirming the absence of target protein expression.
10
11

12 **Cisplatin sensitivity**

13
14 Concentration survival curves were generated with wild-type (WT) HEK-293T and OVCAR8
15
16 cells and compared to each knockout clone using a cell viability assay after 1 hour cDDP
17
18 exposure followed by 96 hour culture in drug-free medium. Figure 2 shows the dose-response
19
20 curves for all the cell lines. Interestingly, different clones from the same parental cell line in
21
22 which the same gene was knocked out showed substantial differences in cDDP sensitivity. With
23
24 1 hour of cDDP exposure the 293T CRT1 KOs had a variable phenotype; whereas KO1 had a
25
26 0.4-fold decrease in IC_{50} , KO2 had a 1.2-fold increase. All of the CTR2, ATOX1, and CCS KOs
27
28 were more sensitive to cDDP compared to the WT HEK-293Ts. The CTR2 KOs had a 0.5- and
29
30 0.4-fold decrease in IC_{50} , while the ATOX1 KOs a 0.7- and 0.4-fold decrease; the CCS KOs had
31
32 a 0.2 and 0.5-fold decrease in IC_{50} value (Figure 2 and Table 3). Collectively, the data suggest
33
34 that knockout of CTR1, CTR2, ATOX1, or CCS modestly increases cDDP sensitivity in the
35
36 HEK-293T cell line.
37
38
39
40
41
42

43
44 Clonal variability was also observed among the OVCAR8 cell lines. The OVCAR8
45
46 CTR1 KOs had a 4.4- and 0.9-fold decrease in IC_{50} , while the CTR2 KOs had a 1.2- and 1.3-fold
47
48 decrease in IC_{50} . The ATOX1 OVCAR8 KOs had a 1.1-fold increase and 0.7-fold decrease in
49
50 IC_{50} , while the CCS KOs had a 0.2 and 0.3-fold decrease (Figure 2 and Table 3). Collectively,
51
52 these results suggest that the effect of CTR1, CTR2, or ATOX1 knockout was variable among
53
54
55
56
57
58
59
60

1
2
3 individual clones and the two cell lines, while knockout of CCS modestly increased cDDP
4
5 sensitivity in both cell types.
6
7

8 Notable variability in cDDP sensitivity was observed among the individual KO clones for
9
10 each gene, suggesting that clonal variability and genetic drift within the population may have a
11
12 large effect. To assess the background variability of the WT population, we isolated 10 sub-
13
14 clones from our transfected HEK-293T and OVCAR8 populations that were negative for
15
16 CRISPR editing (WT gene sequence) and determined their cDDP sensitivity. The IC_{50} values in
17
18 the HEK-293T WT sub-clones ranged from 6.1-50.2 μ M, and 9.1-22.7 μ M in the WT OVCAR8
19
20 sub-clones (Figure 3). These changes in sensitivity are similar to the magnitude changes in our
21
22 knockout clones, indicating that the variability observed in the CTR1, CTR2, ATOX1, and CCS
23
24 KO clones was less than the clonal variability of the starting population in these cell lines.
25
26
27
28

29 **Cellular growth rate**

30
31 The growth rates of the KO clones were compared to the WT cells to assess the impact of protein
32
33 deletion on *in vitro* growth. Previous studies in endothelial cells indicated that silencing of CTR1
34
35 decreased proliferation by 2-fold⁴⁴. ATOX1 and CCS silencing in H1299 lung cancer cells was
36
37 reported to impair cellular growth by decreasing ATP production, decreasing cytochrome c
38
39 oxidase activity, and reducing lipid biosynthesis¹⁸. Cell density was determined as a function of
40
41 time over a period of 7 days in culture and compared among the WT and KO cells. Compared to
42
43 the WT HEK-293T cells, both CTR1 KOs and CTR2 KOs had a slightly decreased rate of
44
45 growth ($p < 0.05$; Figure 4A and 4B). Both ATOX KO1 and KO2 had an increased lag time,
46
47 where the cells took longer to establish growth after passaging; however, once established, these
48
49 cells had a similar cell growth rate compared to the WT cells ($p > 0.05$; Figure 4C). Similarly,
50
51 both CCS KOs had a longer lag time; however, KO1 had a similar rate of growth compared to
52
53
54
55
56
57
58
59
60

1
2
3 WT cells, while KO2 had a 1.2-fold decrease in rate ($p=0.01$) (Figure 4D). Collectively, the
4
5 cellular growth assays showed that all the KO cells are viable in culture and most have similar
6
7 growth rates to the parental cells once they reach a threshold cell density.
8
9

10 **Basal copper levels and copper sensitivity**

11
12 We initially hypothesized that the observed growth defects in the KO lines may be caused by
13
14 defects in Cu homeostasis, such as decreased uptake or failure to shuttle intracellular Cu to
15
16 essential enzymes and cellular compartments. To test this, the total cellular basal Cu content of
17
18 HEK-293T cells was determined by inductively coupled plasmon mass spectrometry (ICP-MS).
19
20 Compared to the WT cells, the CTR1 knockouts had no significant change in basal Cu, while the
21
22 CTR2 KOs had a 1.4 and 1.8-fold increase in Cu ($p=0.06$ and 0.04 , respectively) (Figure 5A).
23
24 ATOX1 protein KO resulted in small 1.2 and 1.3-fold increases in basal Cu level (Figure 5B;
25
26 $p=0.20$ and 0.06 , respectively), which agrees with previous data reported in ATOX1^{-/-} mouse
27
28 embryonic fibroblasts⁴⁵. Strikingly, the CCS KO cells had significantly higher levels of basal Cu
29
30 compared to the WT HEK-293T cells; Cu levels were elevated 1.7-fold in CCS KO1 and 1.5-
31
32 fold in CCS KO2 (Figure 5B; both $p<0.01$), in contrast to previous reports with in which CCS
33
34 was knocked down in MEFs⁴⁶. Thus, the growth defects observed in all the KOs were not
35
36 mediated by defects in total basal cellular Cu.
37
38
39
40
41
42

43
44 Previous reports with ATOX^{-/-} MEFs showed that the knockout cells were more sensitive
45
46 to elevated Cu levels³² due to impaired ATP7B-mediated Cu efflux¹⁴. To test the effect of
47
48 elevated Cu, we repeated the cellular growth experiments using medium supplemented with Cu.
49
50 Cells were grown for 4 days in the presence of medium supplemented with 0-30 μM CuSO₄
51
52 following which cellular viability was quantified. Compared to the WT HEK-293T cells, both
53
54 ATOX1 KOs had a significantly decreased cell viability that correlated with increased
55
56
57
58
59
60

1
2
3 concentrations of Cu ($p < 0.01$ and $= 0.02$; Figure 5E). In contrast, the CTR1, CTR2, and CCS
4
5 KOs had no significant change in viability compared to the WT cells (Figure 5C, D, F; all $p >$
6
7 0.05). These data are consistent with previous findings that ATOX1 deficient cells are sensitive
8
9 to Cu, presumably due to export defects via ATOX1 interactions with ATP7B¹⁴. Moreover,
10
11 these data suggest that the slower growth observed in all the KO cells was not due to a cellular
12
13 Cu deficiency, as even low concentrations of CuSO₄ failed to stimulate growth.
14
15

16 17 **Tumor growth *in vivo***

18
19 Studies have consistently shown that tumors have elevated Cu levels, and that Cu is closely
20
21 associated with key steps in angiogenesis and tumor growth⁴⁷. Cu chelators are effective in
22
23 slowing tumor formation in mice, and the treatment of breast cancer patients with
24
25 tetrathiomolybdate was reported to produce a benefit in survival in a small study⁴⁸. Recent data
26
27 published by Wang *et al.* showed that targeting ATOX1 and CCS with a small molecule
28
29 significantly decreased both lung H1299 and leukemia K562 tumor xenograft growth¹⁸. We
30
31 wondered if any of the individual copper transporters or chaperones is a potential drug target and
32
33 tested the *in vivo* tumorigenicity of our KO cell lines in nude mice.
34
35
36
37

38
39 Xenografts were established by injecting female nu/nu mice subcutaneously with either
40
41 the HEK-293T WT, CTR1, CTR2, or ATOX1 KO cell lines (both knockouts per each gene).
42
43 Tumor growth was measured over a period of 30-45 days, and the logarithmic tumor growth rate
44
45 was compared among the WT and KO cell lines to assess the impact of loss of gene function on
46
47 tumor establishment and growth. The CTR1 KOs had a variable phenotype. CTR1 KO1 had an
48
49 increased lag time and took much longer to establish than KO2 or the WT cells and had a
50
51 significantly decreased growth rate ($p = 0.04$), while KO2 had a slightly increased lag time
52
53 compared to WT, yet a similar growth rate ($p = 0.34$) (Figure 6A). The CTR2 KOs also had a
54
55
56
57
58
59
60

1
2
3 variable phenotype; CTR2 KO1 had a similar lag time and a significantly increased growth rate
4 compared to the WT cells ($p < 0.01$), and CTR2 KO2 had a similar lag time and growth rate ($p =$
5
6 0.91) (Figure 6B). Interestingly, the *in vivo* data for the HEK-293T ATOX1 KOs mirrored the
7
8 cell culture growth results. Compared to the HEK-293T WT cells, both ATOX1 KO cell lines
9
10 had an increased lag time to tumor establishment. However, once the KO tumors were
11
12 established, their growth rate was not different from the WT tumors (Figure 6C; $p = 0.98$ and
13
14 0.51). Thus, targeting ATOX1, CTR1, or CTR2 alone did not appear to be a viable antineoplastic
15
16 therapeutic strategy, as these KO tumors continued to exhibit robust, albeit delayed growth *in*
17
18
19
20
21
22
23
24
25
26
27
28
29
30
31
32
33
34
35
36
37
38
39
40
41
42
43
44
45
46
47
48
49
50
51
52
53
54
55
56
57
58
59
60

Discussion

The Cu homeostasis pathway has been proposed to function as a transport system for cDDP. The effect of CTR1 overexpression and/or knockdown on cDDP uptake and sensitivity has been conflicting. Yeast CTR1 null mutants and mouse CTR1^{-/-} embryonic fibroblasts (MEFs) had increased cDDP resistance and decreased cDDP uptake¹⁹, and re-expression of CTR1 in these MEFs restored cDDP sensitivity⁴⁹. Similarly, overexpression of human CTR1 in SCLC and SR2 cells modestly increased cDDP uptake⁵⁰. However, additional groups reported no correlation between cDDP sensitivity and uptake in cells overexpressing human CTR1^{39, 51}. Our CTR1 KOs did not have a consistent phenotype due to clonal variation. The relatively modest changes in cDDP sensitivity observed here (3 to 4-fold) agree with the previous literature and suggest that CTR1 may not be the primary uptake transport mechanism in HEK-293T and OVCAR8 cell lines.

1
2
3
4
5
6
7
8
9
10
11
12
13
14
15
16
17
18
19
20
21
22
23
24
25
26
27
28
29
30
31
32
33
34
35
36
37
38
39
40
41
42
43
44
45
46
47
48
49
50
51
52
53
54
55
56
57
58
59
60

Whereas CTR1 deletion has been linked with resistance, CTR2 knockdown in MEFs has been reported to increase cDDP uptake and increase cellular sensitivity to cDDP²⁶. CTR2^{-/-} xenograft tumors grew much slower and acquired significantly more cDDP⁵². Similarly, CTR2 knockdown in human 2008 cancer cells rendered the cells 2 to 3-fold hypersensitive to cDDP⁴³. The CTR2 KO cells here had modest, similar-fold changes in cDDP IC₅₀. The HEK-293T KO cells appeared more sensitive while the OVCAR8 KO cells were resistant, possibly due to differences in CTR2 function in varying cell lines.

Several groups have documented direct binding of cDDP to ATOX1 in solution^{30,53} and in cells³¹. *Drosophila* ATOX1 knockout cells were found to be resistant to 1 mM cDDP³³, while ATOX1^{-/-} MEFs had a 1.5-fold increase in IC₅₀³². Because ATOX1 has been shown to directly transfer cDDP to ATP7A and ATP7B in solution^{14,15}, and to modulate Cu detoxification, it may similarly modulate cDDP efflux. Studies regarding direct cDDP transfer between ATOX1 and the metallo-binding domains of ATP7A or ATP7B in solution are conflicting depending on the reducing agent present^{54,55}. Recent studies suggests that Cu binding influences cDDP binding to ATOX1⁵⁶ and may influence transfer of platinum drugs from ATOX1⁵⁷. While ATP7A and ATP7B protein levels were noted to be elevated in cDDP resistant paired cell lines, no changes in ATOX1 expression were seen³⁴. Our ATOX KO cells varied 2-fold in cDDP sensitivity compared to the parental cells. Collectively, these data suggest that ATOX1 is not a major mediator of cDDP toxicity and is not critical to the nuclear import of cDDP. Similar fold changes in cDDP sensitivity were also seen with 96 hour continuous drug exposure assays (data not shown), suggesting that ATOX1 does not mediate cDDP detoxification even though these ATOX1 deficient cells were significantly more sensitive to Cu compared to the other knockouts. However, because ATOX1 and CCS can cross-transfer Cu and are both

1
2
3 present in the nucleus they may have redundant activities. Knockout of both genes may produce
4
5 clearer results; however, deletion of both genes simultaneously may be lethal.
6
7

8 To our knowledge, no reports have described interactions between cDDP and CCS.
9
10 Knockout of CCS in both cell lines in this study resulted in a 2 to 5-fold increase in cDDP
11
12 sensitivity. Previous studies have shown that glutathione (GSH) can compensate for CCS
13
14 deletion to support Cu-mediated SOD1 function ⁵⁸. It's possible that changes in GSH or the
15
16 cellular oxidation state can compensate for the loss of CCS. Additional studies are needed to
17
18 determine whether the changes in cDDP sensitivity seen here are specific or mediated by
19
20 changes in SOD1 activity and ROS balance.
21
22
23

24 This study exposed a major issue with the use of individual KO clones for studies of
25
26 cellular pharmacology. The changes in cDDP sensitivity observed in the KO cells were less than
27
28 those observed between independently isolated wild type clones derived from the parental HEK-
29
30 293T and OVCAR8 populations. However, similar magnitude changes in cDDP sensitivity have
31
32 been reported in cells deficient in DNA damage repair pathways ⁵⁹⁻⁶¹, as well as cDDP resistant
33
34 cells where upregulated ATPase genes important for maintaining tumor cell pH, which
35
36 influences cDDP aquation and activity, were knocked down ⁶². Constant genetic drift of cancer
37
38 cells, especially cells in tissue culture, pose a challenge to the use of isogenic knockout clones to
39
40 assess the effect of loss of function of a given gene. The clonal variability observed in this study
41
42
43
44
45
46 mandates the use of numerous knockout clones in future studies.
47

48 It is important to note that variation in drug sensitivity among the knockouts may be
49
50 mediated by off-target CRISPR-Cas9 editing. Cas9 mutants with increased fidelity have now
51
52 been engineered that have off-target effects below the limit of detection ^{63, 64}. Improvements in
53
54
55
56 Cas9 design may allow for bulk sorting of a transfected population to more rapidly study the
57
58
59
60

1
2
3 effects of gene editing and protein deletion, thus bypassing the arduous task of characterizing
4 individual clones.
5
6
7
8
9

10 **Conclusion**

11
12
13 The mechanisms of cDDP uptake and transport remain largely unknown, despite
14 widespread clinical use as an anti-neoplastic agent for the past 50 years. Initial studies described
15 correlations between cDDP response and patient survival with copper transport protein
16 expression, suggesting that the two metals may utilize similar pathways to enter and traffic
17 through cells. However, protein knockdown studies in cells from several species have been
18 conflicting. The generation of isogenic knockout cell lines in 4 Cu transport/chaperones genes
19 represents a clean system to address this question.
20
21
22
23
24
25
26
27
28

29
30 Knockout of any of the 4 genes reported here resulted in variable changes in sensitivity to
31 cDDP. The fold changes range from 2 to 5-fold. However, our data indicate that knockout of
32 these Cu transporters and chaperones failed to produce changes in cDDP sensitivity that were
33 greater than the variance in cDDP sensitivity observed among non-edited clones isolated from
34 the same parental population. The mechanisms of cellular entry and nuclear translocation of
35 cDDP remain unknown. Genome-wide CRISPR-Cas9 screens directed at identifying genes that
36 modulate cDDP sensitivity are currently underway.
37
38
39
40
41
42
43
44
45
46
47

48 **Acknowledgements**

49
50
51 This work was supported by grants R01-CA152185 and T32CA121938 from the National
52 Institutes of Health. We would like to thank Professor James Day the Scripps Institute of
53 Oceanography for his help with ICP-MS.
54
55
56
57
58
59
60

References

1. P. Abada and S. B. Howell, Regulation of cisplatin cytotoxicity by Cu influx transporters, *Met Based Drugs*, 2010, **2010**, 317581.
2. C. J. De Feo, S. G. Aller and V. M. Unger, A structural perspective on copper uptake in eukaryotes, *Biometals*, 2007, **20**, 705-716.
3. C. J. De Feo, S. G. Aller, G. S. Siluvai, N. J. Blackburn and V. M. Unger, Three-dimensional structure of the human copper transporter hCTR1, *Proc Natl Acad Sci USA*, 2009, **106**, 4237-4242.
4. I. F. Tsigelny, Y. Sharikov, J. P. Greenberg, M. A. Miller, V. L. Kouznetsova, C. A. Larson and S. B. Howell, An All-Atom Model of the Structure of Human Copper Transporter 1, *Cell Biochem Biophys*, 2012, **63**, 223-234.
5. S. A. Molloy and J. H. Kaplan, Copper-dependent recycling of hCTR1, the human high affinity copper transporter, *J Biol Chem*, 2009, **284**, 29704-29713.
6. H. Ohrvik, Y. Nose, L. K. Wood, B. E. Kim, S. C. Gleber, M. Ralle and D. J. Thiele, Ctr2 regulates biogenesis of a cleaved form of mammalian Ctr1 metal transporter lacking the copper- and cisplatin-binding ecto-domain, *Proc Natl Acad Sci USA*, 2013, **110**, E4279-4288.
7. P. V. van den Berghe, D. E. Folmer, H. E. Malingre, E. van Beurden, A. E. Klomp, B. van de Sluis, M. Merckx, R. Berger and L. W. Klomp, Human copper transporter 2 is localized in late endosomes and lysosomes and facilitates cellular copper uptake, *Biochem J*, 2007, **407**, 49-59.

- 1
2
3 8. E. M. Rees and D. J. Thiele, Identification of a vacuole-associated metalloreductase and
4 its role in CTR2-mediated intracellular copper mobilization, *J Biol Chem*, 2007, **282**,
5 21629 - 21638.
6
7
- 8
9
10 9. M. E. Portnoy, P. J. Schmidt, R. S. Rogers and V. C. Culotta, Metal transporters that
11 contribute copper to metallochaperones in *Saccharomyces cerevisiae*, *Mol Genet*
12 *Genomics*, 2001, **265**, 873-882.
13
14
- 15
16
17 10. H. Ohrvik, B. Logeman, G. Noguchi, I. Eriksson, L. Kjellen, D. J. Thiele and G. Pejler,
18 Ctr2 Regulates Mast Cell Maturation by Affecting the Storage and Expression of
19 Tryptase and Proteoglycans, *J Immunol*, 2015, **195**, 3654-3664.
20
21
- 22
23
24 11. C. Y. Tsai, J. K. Liebig, I. F. Tsigelny and S. B. Howell, The copper transporter 1
25 (CTR1) is required to maintain the stability of copper transporter 2 (CTR2), *Metalloomics*,
26 2015, **7**, 1477-1487.
27
28
- 29
30
31 12. V. C. Culotta, L. W. Klomp, J. Strain, R. L. Casareno, B. Krems and J. D. Gitlin, The
32 copper chaperone for superoxide dismutase, *J Biol Chem*, 1997, **272**, 23469-23472.
33
34
- 35
36
37 13. P. C. Wong, D. Waggoner, J. R. Subramaniam, L. Tessarollo, T. B. Bartnikas, V. C.
38 Culotta, D. L. Price, J. Rothstein and J. D. Gitlin, Copper chaperone for superoxide
39 dismutase is essential to activate mammalian Cu/Zn superoxide dismutase, *Proc Natl*
40 *Acad Sci USA*, 2000, **97**, 2886-2891.
41
42
- 43
44
45 14. I. Hamza, J. Prohaska and J. D. Gitlin, Essential role for Atox1 in the copper-mediated
46 intracellular trafficking of the Menkes ATPase, *Proc Natl Acad Sci USA*, 2003, **100**,
47 1215-1220.
48
49
50
51
52
53
54
55
56
57
58
59
60

- 1
2
3
4
5
6
7
8
9
10
11
12
13
14
15
16
17
18
19
20
21
22
23
24
25
26
27
28
29
30
31
32
33
34
35
36
37
38
39
40
41
42
43
44
45
46
47
48
49
50
51
52
53
54
55
56
57
58
59
60
15. I. Hamza, M. Schaefer, L. Klomp and J. Gitlin, Interaction of the copper chaperone HAH1 with the Wilson disease protein is essential for copper homeostasis., *Proc Natl Acad Sci USA*, 1999, **96**, 13363-13368.
 16. S. Itoh, H. W. Kim, O. Nakagawa, K. Ozumi, S. M. Lessner, H. Aoki, K. Akram, R. D. McKinney, M. Ushio-Fukai and T. Fukai, Novel role of antioxidant-1 (atox1) as a copper dependent transcription factor involved in cell proliferation, *J Biol Chem*, 2008, **283**, 9157-9167.
 17. S. Petzoldt, D. Kahra, M. Kovermann, A. P. Dingeldein, M. S. Niemiec, J. Aden and P. Wittung-Stafshede, Human cytoplasmic copper chaperones Atox1 and CCS exchange copper ions in vitro, *Biometals*, 2015, **28**, 577-585.
 18. J. Wang, C. Luo, C. Shan, Q. You, J. Lu, S. Elf, Y. Zhou, Y. Wen, J. L. Vinkenborg, J. Fan, H. Kang, R. Lin, D. Han, Y. Xie, J. Karpus, S. Chen, S. Ouyang, C. Luan, N. Zhang, H. Ding, M. Merckx, H. Liu, J. Chen, H. Jiang and C. He, Inhibition of human copper trafficking by a small molecule significantly attenuates cancer cell proliferation, *Nature Chem*, 2015, **7**, 968-979.
 19. S. Ishida, J. Lee, D. J. Thiele and I. Herskowitz, Uptake of the anticancer drug cisplatin mediated by the copper transporter Ctr1 in yeast and mammals, *Proc Natl Acad Sci USA*, 2002, **99**, 14298-14302.
 20. X. Lin, T. Okuda, A. Holzer and S. B. Howell, The copper transporter CTR1 regulates cisplatin uptake in *saccharomyces cerevisiae*, *Mol Pharmacol*, 2002, **62**, 1154-1159.
 21. S. Ishida, F. McCormick, K. Smith-McCune and D. Hanahan, Enhancing Tumor-Specific Uptake of the Anticancer Drug Cisplatin with a Copper Chelator, *Cancer Cell*, 2010, **17**, 574-583.

- 1
2
3
4
5
6
7
8
9
10
11
12
13
14
15
16
17
18
19
20
21
22
23
24
25
26
27
28
29
30
31
32
33
34
35
36
37
38
39
40
41
42
43
44
45
46
47
48
49
50
51
52
53
54
55
56
57
58
59
60
22. Z. D. Liang, Y. Long, W. B. Tsai, S. Fu, R. Kurzrock, M. Gagea-Iurascu, F. Zhang, H. H. Chen, B. T. Hennessy, G. B. Mills, N. Savaraj and M. T. Kuo, Mechanistic basis for overcoming platinum resistance using copper chelating agents, *Mol Cancer Ther*, 2012, **11**, 2483-2494.
23. H. H. Chen, J. J. Yan, W. C. Chen, M. T. Kuo, Y. H. Lai, W. W. Lai, H. S. Liu and W. C. Su, Predictive and prognostic value of human copper transporter 1 (hCtr1) in patients with stage III non-small-cell lung cancer receiving first-line platinum-based doublet chemotherapy, *Lung Cancer*, 2012, **75**, 228-234.
24. Y. Y. Lee, C. H. Choi, I. G. Do, S. Y. Song, W. Lee, H. S. Park, T. J. Song, M. K. Kim, T. J. Kim, J. W. Lee, D. S. Bae and B. G. Kim, Prognostic value of the copper transporters, CTR1 and CTR2, in patients with ovarian carcinoma receiving platinum-based chemotherapy, *Gynecol Oncol*, 2011, **122**, 361-365.
25. H. Yoshida, M. Teramae, M. Yamauchi, T. Fukuda, T. Yasui, T. Sumi, K. Honda and O. Ishiko, Association of copper transporter expression with platinum resistance in epithelial ovarian cancer, *Anticancer Res*, 2013, **33**, 1409-1414.
26. B. G. Blair, C. A. Larson, R. Safaei and S. B. Howell, Copper transporter 2 regulates the cellular accumulation and cytotoxicity of cisplatin and carboplatin, *Clin Cancer Res*, 2009, **15**, 4312-4321.
27. B. Blair, C. Larson, P. Adams, P. Abada, R. Safaei and S. Howell, Regulation of copper transporter 2 expression by copper and cisplatin in human ovarian carcinoma cells, *Mol Pharmacol*, 2010, **77**, 912 - 921.

- 1
2
3
4 28. L. Zhao, Q. Cheng, Z. Wang, Z. Xi, D. Xu and Y. Liu, Cisplatin binds to human copper
5 chaperone Cox17: the mechanistic implication of drug delivery to mitochondria, *Chem*
6
7
8 *Commun (Camb)*, 2014, **50**, 2667-2669.
9
- 10 29. A. K. Boal and A. C. Rosenzweig, Crystal structures of cisplatin bound to a human
11
12 copper chaperone, *J Am Chem Soc*, 2009, **131**, 14196-14197.
13
- 14 30. V. Calandrini, T. H. Nguyen, F. Arnesano, A. Galliani, E. Ippoliti, P. Carloni and G.
15
16 Natile, Structural biology of cisplatin complexes with cellular targets: the adduct with
17
18 human copper chaperone atox1 in aqueous solution, *Chemistry*, 2014, **20**, 11719-11725.
19
- 20 31. M. E. Palm-Espling, C. Lundin, E. Bjorn, P. Naredi and P. Wittung-Stafshede, Interaction
21
22 between the Anticancer Drug Cisplatin and the Copper Chaperone Atox1 in Human
23
24 Melanoma Cells, *Protein Pept Lett*, 2014, **21**, 63-68.
25
26
- 27 32. R. Safaei, M. H. Maktabi, B. G. Blair, C. A. Larson and S. B. Howell, Effects of the loss
28
29 of Atox1 on the cellular pharmacology of cisplatin, *J Inorg Biochem*, 2009, **103**, 333-341.
30
31
- 32 33. H. Hua, V. Gunther, O. Georgiev and W. Schaffner, Distorted copper homeostasis with
33
34 decreased sensitivity to cisplatin upon chaperone Atox1 deletion in *Drosophila*,
35
36
37 *Biometals*, 2011, **24**, 445-453.
38
- 39 34. K. Katano, A. Kondo, R. Safaei, A. Holzer, G. Samimi, M. Mishima, Y. M. Kuo, M.
40
41 Rochdi and S. B. Howell, Acquisition of resistance to cisplatin is accompanied by
42
43 changes in the cellular pharmacology of copper, *Cancer Res*, 2002, **62**, 6559-6565.
44
45
- 46 35. L. S. Mangala, V. Zuzel, R. Schmandt, E. S. Leshane, J. B. Halder, G. N. Armaiz-Pena,
47
48 W. A. Spannuth, T. Tanaka, M. M. Shahzad, Y. G. Lin, A. M. Nick, C. G. Danes, J. W.
49
50 Lee, N. B. Jennings, P. E. Vivas-Mejia, J. K. Wolf, R. L. Coleman, Z. H. Siddik, G.
51
52
53
54
55
56
57
58
59
60

- 1
2
3 Lopez-Berestein, S. Lutsenko and A. K. Sood, Therapeutic Targeting of ATP7B in
4 Ovarian Carcinoma, *Clin Cancer Res*, 2009, **15**, 3770-3780.
5
6
7
8 36. K. Yoshizawa, S. Nozaki, H. Kitahara, T. Ohara and e. al, Copper efflux transporter
9 (ATP7B) contributes to acquisition of cisplatin-resistance in human oral squamous cell
10 lines, *Oncol Rep*, 2007, **18**, 987-991.
11
12
13 37. M. Komatsu, T. Sumizawa, M. Mutoh, Z.-S. Chen, K. Terada, T. Furukawa, X.-L. Yang,
14 H. Gao, N. Miura, T. Sugiyama and S. Akiyama, Copper-transporting P-type adenosine
15 triphosphatase (ATP7B) is associated with cisplatin resistance, *Cancer Res*, 2000, **60**,
16 1312-1316.
17
18
19 38. V. Calandrini, F. Arnesano, A. Galliani, T. H. Nguyen, E. Ippoliti, P. Carloni and G.
20 Natile, Platination of the copper transporter ATP7A involved in anticancer drug
21 resistance, *Dalton Trans*, 2014, **43**, 12085-12094.
22
23
24 39. K. D. Ivy and J. H. Kaplan, A re-evaluation of the role of hCTR1, the human high-
25 affinity copper transporter, in platinum-drug entry into human cells, *Mol Pharmacol*,
26 2013, **83**, 1237-1246.
27
28
29 40. E. B. Maryon, S. A. Molloy, A. M. Zimnicka and J. H. Kaplan, Copper entry into human
30 cells: progress and unanswered questions, *Biometals*, 2007, **20**, 355-364.
31
32
33 41. F. A. Ran, P. D. Hsu, J. Wright, V. Agarwala, D. A. Scott and F. Zhang, Genome
34 engineering using the CRISPR-Cas9 system, *Nat Protoc*, 2013, **8**, 2281-2308.
35
36
37 42. M. T. Kuo, Overcoming cisplatin-resistance by copper-lowering agents, *Mol Cancer*
38 *Ther*, 2012, **11**, 1221-1225.
39
40
41
42
43
44
45
46
47
48
49
50
51
52
53
54
55
56
57
58
59
60

- 1
2
3
4 43. C. P. Huang, M. Fofana, J. Chan, C. J. Chang and S. B. Howell, Copper Transporter 2
5
6 Regulates Intracellular Copper and Sensitivity to Cisplatin, *Metalloomics*, 2014, **26**, 654-
7
8 661.
9
10
11 44. G. Narayanan, B. S. R, H. Vuyyuru, B. Muthuvel and S. Konerirajapuram Natrajan,
12
13 CTR1 Silencing Inhibits Angiogenesis by Limiting Copper Entry into Endothelial Cells,
14
15 *PLoS One*, 2013, **8**, e71982.
16
17
18 45. R. McRae, B. Lai and C. J. Fahrni, Copper redistribution in Atox1-deficient mouse
19
20 fibroblast cells, *J Biol Inorg Chem*, 2010, **15**, 99-105.
21
22
23 46. T. Miyayama, Y. Ishizuka, T. Iijima, D. Hiraoka and Y. Ogra, Roles of copper chaperone
24
25 for superoxide dismutase 1 and metallothionein in copper homeostasis, *Metalloomics*,
26
27 2011, **3**, 693-701.
28
29
30 47. G. F. Chen, V. Sudhahar, S. W. Youn, A. Das, J. Cho, T. Kamiya, N. Urao, R. D.
31
32 McKinney, B. Surenkhuu, T. Hamakubo, H. Iwanari, S. Li, J. W. Christman, S.
33
34 Shantikumar, G. D. Angelini, C. Emanuelli, M. Ushio-Fukai and T. Fukai, Copper
35
36 Transport Protein Antioxidant-1 Promotes Inflammatory Neovascularization via
37
38 Chaperone and Transcription Factor Function, *Sci Rep*, 2015, **5**, 14780.
39
40
41 48. S. Jain, J. Cohen, M. M. Ward, N. Kornhauser, E. Chuang, T. Cigler, A. Moore, D.
42
43 Donovan, C. Lam, M. V. Cobham, S. Schneider, S. M. Hurtado Rua, S. Benkert, C.
44
45 Mathijssen Greenwood, R. Zelkowitz, J. D. Warren, M. E. Lane, V. Mittal, S. Rafii and L.
46
47 T. Vahdat, Tetrathiomolybdate-associated copper depletion decreases circulating
48
49 endothelial progenitor cells in women with breast cancer at high risk of relapse, *Ann*
50
51 *Oncol*, 2013, **24**, 1491-1498.
52
53
54
55
56
57
58
59
60

- 1
2
3
4
5
6
7
8
9
10
11
12
13
14
15
16
17
18
19
20
21
22
23
24
25
26
27
28
29
30
31
32
33
34
35
36
37
38
39
40
41
42
43
44
45
46
47
48
49
50
51
52
53
54
55
56
57
58
59
60
49. C. A. Larson, B. G. Blair, R. Safaei and S. B. Howell, The Role of the Mammalian Copper Transporter 1 in the Cellular Accumulation of Platinum-based Drugs, *Mol Pharmacol*, 2009, **75**, 324-330.
50. I. Song, N. Savaraj, Z. Siddik, P. Liu, Y. Wei, C. Wu and M. Kuo, Role of copper transporter Ctr1 in the transport of platinum-based antitumor agents in cisplatin-sensitive and resistant cells, *Mol Cancer Ther*, 2004, **3** 1543-1549.
51. G. L. Beretta, L. Gatti, S. Tinelli, E. Corna, D. Colangelo, F. Zunino and P. Perego, Cellular pharmacology of cisplatin in relation to the expression of human copper transporter CTR1 in different pairs of cisplatin-sensitive and -resistant cells, *Biochem Pharmacol*, 2004, **68**, 283-291.
52. B. G. Blair, C. A. Larson, P. L. Adams, P. B. Abada, C. E. Pesce, R. Safaei and S. Howell, Copper Transporter 2 regulates endocytosis and controls tumor growth and sensitivity to cisplatin in vivo, *Mol Pharmacol*, 2011, **79**, 157-166.
53. M. E. Palm, C. F. Weise, C. Lundin, G. Wingsle, Y. Nygren, E. Bjorn, P. Naredi, M. Wolf-Watz and P. Wittung-Stafshede, Cisplatin binds human copper chaperone Atox1 and promotes unfolding in vitro, *Proc Natl Acad Sci USA*, 2011, **108**, 6951-6956.
54. A. Galliani, M. Losacco, A. Lasorsa, G. Natile and F. Arnesano, Cisplatin handover between copper transporters: the effect of reducing agents, *J Biol Inorg Chem*, 2014, DOI: 10.1007/s00775-014-1138-1.
55. N. V. Dolgova, S. Nokhrin, C. H. Yu, G. N. George and O. Y. Dmitriev, Copper chaperone Atox1 interacts with the metal-binding domain of Wilson disease protein in cisplatin detoxification, *Biochem J*, 2013, **454**, 147-156.

- 1
2
3
4
5
6
7
8
9
10
11
12
13
14
15
16
17
18
19
20
21
22
23
24
25
26
27
28
29
30
31
32
33
34
35
36
37
38
39
40
41
42
43
44
45
46
47
48
49
50
51
52
53
54
55
56
57
58
59
60
56. Z. Xi, W. Guo, C. Tian, F. Wang and Y. Liu, Copper binding promotes the interaction of cisplatin with human copper chaperone Atox1, *Chem Commun (Camb)*, 2013, **49**, 11197-11199.
57. Z. Xi, W. Guo, C. Tian, F. Wang and Y. Liu, Copper binding modulates the platination of human copper chaperone Atox1 by antitumor trans-platinum complexes, *Metalloomics*, 2014, **6**, 491-497.
58. M. C. Carroll, J. B. Girouard, J. L. Ulloa, J. R. Subramaniam, P. C. Wong, J. S. Valentine and V. C. Culotta, Mechanisms for activating Cu- and Zn-containing superoxide dismutase in the absence of the CCS Cu chaperone, *Proc Natl Acad Sci USA*, 2004, **101**, 5964-5969.
59. F. J. Djit, A. M. J. Fichtinger-Schepman, F. Berends and J. Reedijk, Formation and repair of cisplatin-induced adducts to DNA in cultured normal and repair-deficient human fibroblasts, *Cancer Res*, 1988, **48**, 6058-6062.
60. A. C. Plooy, M. van Dijk, F. Berends and P. H. Lohman, Formation and repair of DNA interstrand cross-links in relation to cytotoxicity and unscheduled DNA synthesis induced in control and mutant human cells treated with cis-diamminedichloroplatinum(II), *Cancer Res*, 1985, **45**, 4178-4184.
61. E. H. A. Poll, P. J. Abrahams, F. Arwert and A. W. Eriksson, Host-cell reactivation of cis-diamminedichloroplatinum (II)- treated SV40 DNA in normal human, Fanconi anaemia and xeroderma pigmentosum fibroblasts, *Mutation Res*, 1984, **132**, 181-187.
62. A. Kulshrestha, G. K. Katara, J. Ginter, S. Pamarthy, S. A. Ibrahim, M. K. Jaiswal, C. Sandulescu, R. Periakaruppan, J. Dolan, A. Gilman-Sachs and K. D. Beaman, Selective

- 1
2
3 inhibition of tumor cell associated Vacuolar-ATPase 'a2' isoform overcomes cisplatin
4 resistance in ovarian cancer cells, *Mol Oncol*, 2016, DOI: 10.1016/j.molonc.2016.01.003.
5
6
7
8 63. B. P. Kleinstiver, V. Pattanayak, M. S. Prew, S. Q. Tsai, N. T. Nguyen, Z. Zheng and J.
9 K. Joung, High-fidelity CRISPR-Cas9 nucleases with no detectable genome-wide off-
10 target effects, *Nature*, 2016, **529**, 490-495.
11
12
13 64. I. M. Slaymaker, L. Gao, B. Zetsche, D. A. Scott, W. X. Yan and F. Zhang, Rationally
14 engineered Cas9 nucleases with improved specificity, *Science*, 2015, **351**, 84-88.
15
16
17
18
19
20
21
22
23
24
25
26
27
28
29
30
31
32
33
34
35
36
37
38
39
40
41
42
43
44
45
46
47
48
49
50
51
52
53
54
55
56
57
58
59
60

Figure Legends

Figure 1. Western blot analysis of clones in which CTR1, CTR2, ATOX1, and CCS were knocked out. Basal protein expression levels in the wild type (WT) HEK293T and OVCAR8 and the knockout (KO) clones. A, CTR1; B, CTR2; C, ATOX1; and, D, CCS.

Figure 2. cDDP concentration-survival curves for the wild type HEK293T and OVCAR8 cell lines and each of the knockout clones. Cells were seeded in 96 well plates and treated with 0-100 μ M cDDP for 1 h and then incubated in drug-free medium for an additional 4 days. The data represent the mean \pm SEM of three independent experiments plated in sextuplicate for each drug concentration. For all cell lines circles (\bullet , solid line) represent WT, squares represent KO1 (\blacksquare , dashed line), and triangles (\blacktriangle , dotted line) represent KO2.

Figure 3. cDDP concentration-survival curves for ten wild type HEK293T or OVCAR8 subclones. Ten subclones were sorted from the parental population. Cells were seeded in 96 well plates and treated with 0-100 μ M cDDP for 1 h and then incubated in drug-free medium for an additional 4 days. The data represent the mean \pm SEM of two independent experiments plated in sextuplicate for each drug concentration.

Figure 4. Growth rates of the parental HEK-293T and knockout cells in culture. A) CTR1, B) CTR2, C) ATOX1, and D) CCS. Cells were seeded in 96 well plates and cell viability was quantified every 24 hours. The data were log₁₀ transformed and the linear data

1
2
3 for cell growth were fit with a linear trend line shown. All data represent the mean \pm
4 SEM of three independent experiments plated in quadruplicate. For all cell lines
5
6 circles (●, solid line) represent WT, squares represent KO1 (■, dashed line), and
7
8 triangles (▲, dotted line) represent KO2.
9
10
11
12
13
14

15 Figure 5. Copper homeostasis in HEK-293T parental and knockout cell lines. A, B) Basal
16 whole cell Cu concentrations in the wild-type (WT) and all knockout (KO) cell lines.
17
18 P-value WT vs.: CTR1 KO1 = 0.62; CTR1 KO2 = 0.09; CTR2 KO1 = 0.06; CTR2
19
20 KO2 = 0.04. P-value WT vs.: ATOX KO1 = 0.02; ATOX1 KO2 = 0.06; CCS KO1
21
22 <0.01; CCS KO2 <0.01. Cells were plated in in 6-well plates, and each well was
23
24 harvested for basal Cu quantification with ICP-MS. Copper concentrations were
25
26 normalized to the average total protein concentration from a second 6-well plate. The
27
28 data represent the mean \pm SEM of three independent experiments plated in
29
30 sextuplicate. C-F) Cu sensitivity stress test in the C) 293T CTR1 knockout cell lines,
31
32 D) 293T CTR2 KO cell lines, E) 293T ATOX1 KO cell lines, and F) 293T CCS KO
33
34 cell lines. For all cell lines circles (●, solid line) represent WT, squares represent
35
36 KO1 (■, dashed line), and triangles (▲, dotted line) represent KO2. Cells were plated
37
38 in 96 well plates in media supplemented with 0-30 μ M CuSO₄ and incubation in
39
40 culture for 4 days. The data represent the mean \pm SEM for three independent
41
42 experiments plated in triplicate.
43
44
45
46
47
48
49
50
51
52

53 Figure 6. HEK-293T wild type and CTR1, CTR2, and ATOX1 knockout tumor growth in nude
54
55 mice. Six-week old female nu/nu mice were injected with 1×10^6 cells. Tumor growth
56
57
58
59
60

1
2
3 was measured over a period of 30-50 days and log10 transformed. A) CTR1 KOs, B)
4 CTR2 KOs, and C) ATOX1 KOs. For all cell lines circles (●, solid line) represent
5 WT, squares represent KO1 (■, dashed line), and triangles (▲, dotted line) represent
6 KO2. The linear growth rates of the transformed data were calculated and statistically
7 compared among the 293T WT and KO cell lines. N=5-8 tumors CTR1, 8 tumors
8 CTR2, and 15-16 tumors for ATOX1.
9
10
11
12
13
14
15
16
17
18
19
20
21
22
23
24
25
26
27
28
29
30
31
32
33
34
35
36
37
38
39
40
41
42
43
44
45
46
47
48
49
50
51
52
53
54
55
56
57
58
59
60

Table 1. DNA allele sequences of the ATOX1 and CCS knockout cell lines generated with CRISPR-Cas9 targeting technology.

Cell Line	Allele 1 nucleotide sequence	Allele 2 nucleotide sequence
ATOX1 (Exon 2 Targeted CRISPR site)		
ATOX1 WT	GCTGAAGCTGTCTCTCGGGTCCTCAATAAGCTTGGAGGTGAGTGAGTGG	
HEK-293T ATOX1 KO1	GCTGAAGCTGTCTCTCGGGTCCTCAATAA <u>A</u> GCTTGGAGGTGAGTGAGTGG (+1 nt)	
HEK-293T ATOX1 KO2	GCTGAAGCTGTCTCTCGGGTC ----- GCTTGGAGGTGAGTGAGTGG (Δ8 nt)	
OVCAR8 ATOX1 KO1	G ----- ----- -----AGTGAGTGG (Δ39 nt)	GCTGAAG ----- ----- ----- G (Δ41 nt)
OVCAR8 ATOX1 KO2	GCTGAAGCTGTCTCTCGGGTCCTCAA TAA <u>A</u> GCTT GGAGGTGAGTGAGTGG (+1 nt)	GCTGAAGCTGTCTCTCGGGTCCTCA ATA- GCTT GGAGGTGAGTGAGTGG (Δ1 nt)
CCS (Exon 1 Targeted CRISPR site)		
CCS WT	GGGTCCAGAATGGCTTCGGATTCGGGGAACCAGGGG	
HEK-293T CCS KO1	GGGTCCAGAATGGCTTCGGA TTCGGGG – ACCAGGGG (Δ 1 nt)	GGG ----- ----- GG (Δ 31 nt)
HEK-293T CCS KO2	GGGTCCAGAATGGCTTCGGA TTCGGGG – ACCAGGGG (Δ 1 nt)	GGGTCCAGAATGGCTTCGGA TTCGGG - - ACCAGGGG (Δ 2 nt)
OVCAR8 CCS KO1	GGGTCCAGAATGGCTTCGGA TTCGGGG – ACCAGGGG (Δ 1 nt)	GGGTCCAGAATGGCTTCGGA TTCGGGGAA – CAGGGG (Δ 1 nt)
OVCAR8 CCS KO2	GGGTCCAGAATGGCTTCGGA TTCGGGG – ACCAGGGG (Δ 1 nt)	GGGTCCAGAATGG ----- ----- G (Δ 22 nt)

Table 2. Predicted protein amino acid sequences of the ATOX1 and CCS knockout cell lines.

Cell Line	Allele 1 amino acid sequence	Allele 2 amino acid sequence
ATOX1		
ATOX1 WT	MPKHEFSVDMTCGGCAEAVSRVLNKLGGVKYDIDLPNKKVCIESEHSMDTLLATLKKTG KTVSYLGLE	
HEK-293T ATOX1 KO1	MPKHEFSVDMTCGGCAEAVSRVLNKAWRS*	
HEK-293T ATOX1 KO2	MPKHEFSVDMTCGGCAEAVSRVAWRS*	
OVCAR8 ATOX1 KO1	n/a [§]	n/a [§]
OVCAR8 ATOX1 KO2	MPKHEFSVDMTCGGCAEAVSRVLNK AWRS*	MPKHEFSVDMTCGGCAEAVSRVLNSLEELSM TLTCPTRRSALNLSTAWTLCLQP [†]
CCS		
CCS WT	MASDSGNQGTLCLEFAVQMTQCSCVDAVRKSLQGAVGVQDVEVHLEDQMVLVHTTL PSQEVQALLEGTGRQAVLKGMGSGQLQNLGAAVAILGGPGTVQGVVRFLLQTPERCLIE GTIDGLEPGLHGLHVHQYGDLTNNCNSCGNHFNPDGASHGGPQSDRHRGDLGNVRAD ADGRAIFRMEDEQLKVDVIGRSLIIDEGEDDLGRGGHPLSKITGNSGERLACGIIARSAG LFQNPQKQICSDGLTIWEERGRPIAGKGRKESAQPPAHL	
HEK-293T CCS KO1	MASDSGTRGPSARWSSRCR*	n/a [‡]
HEK-293T CCS KO2	MASDSGTRGPSARWSSRCR*	MASDSGPGDPLHVGVRGADDLSELCGRGAQI PARGGRCPCGGALGGPDGLGTHHSTQPGGA GSPGRHGAAGGTQGHGQRPVAESGGSSGHPG GAWHRAGGGALPTADP [†]
OVCAR8 CCS KO1	MASDSGTRGPSARWSSRCR*	MASDSGNRGPSARWSSRCR*
OVCAR8 CCS KO2	MASDSGTRGPSARWSSRCR*	MGPSARWSSRCR*

*Early stop codon causes translation termination

[†]Sequence shows less than 50% homology to WT protein

[‡]CRISPR induced lesion removes translation start codon

[§]CRISPR induced lesion removes exon/intron boundary; is predicted to impair mRNA splicing.

Table 3. Cisplatin IC₅₀ values.

	HEK-293T			OVCAR8		
	IC ₅₀ (μM) mean ± SEM*	Fold change	P-value	IC ₅₀ (μM) mean ± SEM*	Fold change	P-value
WT	53.1 ± 3.3	-	-	25.6 ± 4.5	-	-
CTR1/KO1	19.3 ± 1.0	0.4	0.412	112.3 ± 25.9	4.4	0.341
CTR1/KO2	65.3 ± 4.5	1.2	0.408	23.6 ± 2.6	0.9	0.165
CTR2/KO1	26.1 ± 0.3	0.5	0.043	31.5 ± 7.9	1.2	0.915
CTR2/KO2	21.9 ± 0.1	0.4	<0.01	34.4 ± 11.8	1.3	0.398
ATOX1/KO1	36.8 ± 8.4	0.7	0.440	26.9 ± 1.8	1.1	0.025
ATOX1/KO2	20.7 ± 1.9	0.4	<0.01	17.2 ± 4.0	0.7	0.287
CCS/KO1	10.5 ± 1.8	0.2	0.047	5.6 ± 0.6	0.2	<0.01
CCS/KO2	26.9 ± 5.5	0.5	0.214	8.2 ± 0.7	0.3	0.04

*The data represent the mean ± SEM of at least three independent experiments plated in sextuplicate

1
2
3
4
5
6
7
8
9
10
11
12
13
14
15
16
17
18
19
20
21
22
23
24
25
26
27
28
29
30
31
32
33
34
35
36
37
38
39
40
41
42
43
44
45
46
47
48
49

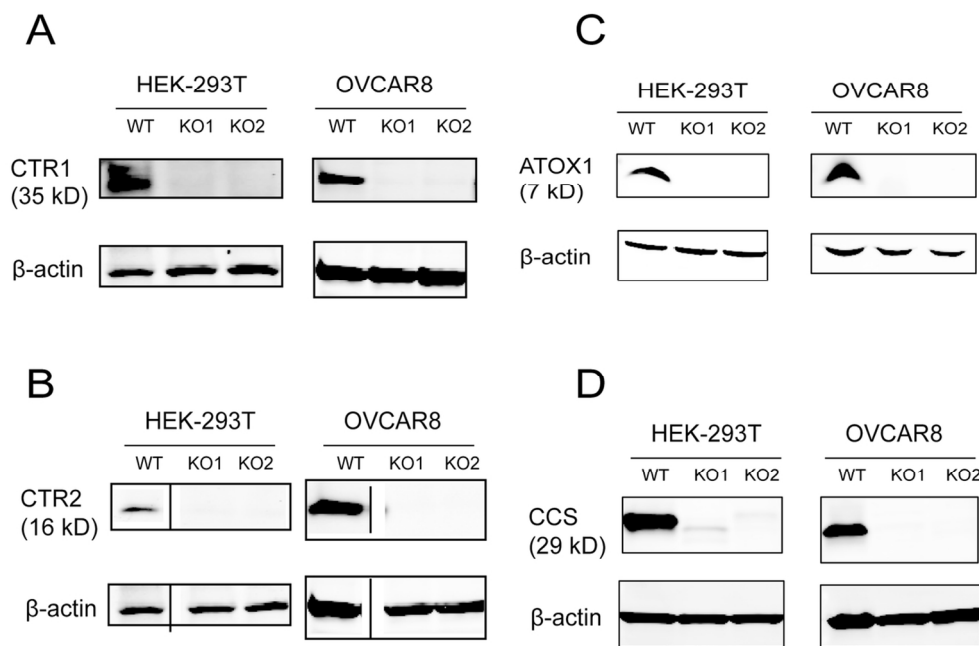


Figure 1. Western blot analysis of clones in which CTR1, CTR2, ATOX1, and CCS were knocked out. Basal protein expression levels in the wild type (WT) HEK293T and OVCAR8 and the knockout (KO) clones. A, CTR1; B, CTR2; C, ATOX1; and, D, CCS.
113x76mm (300 x 300 DPI)

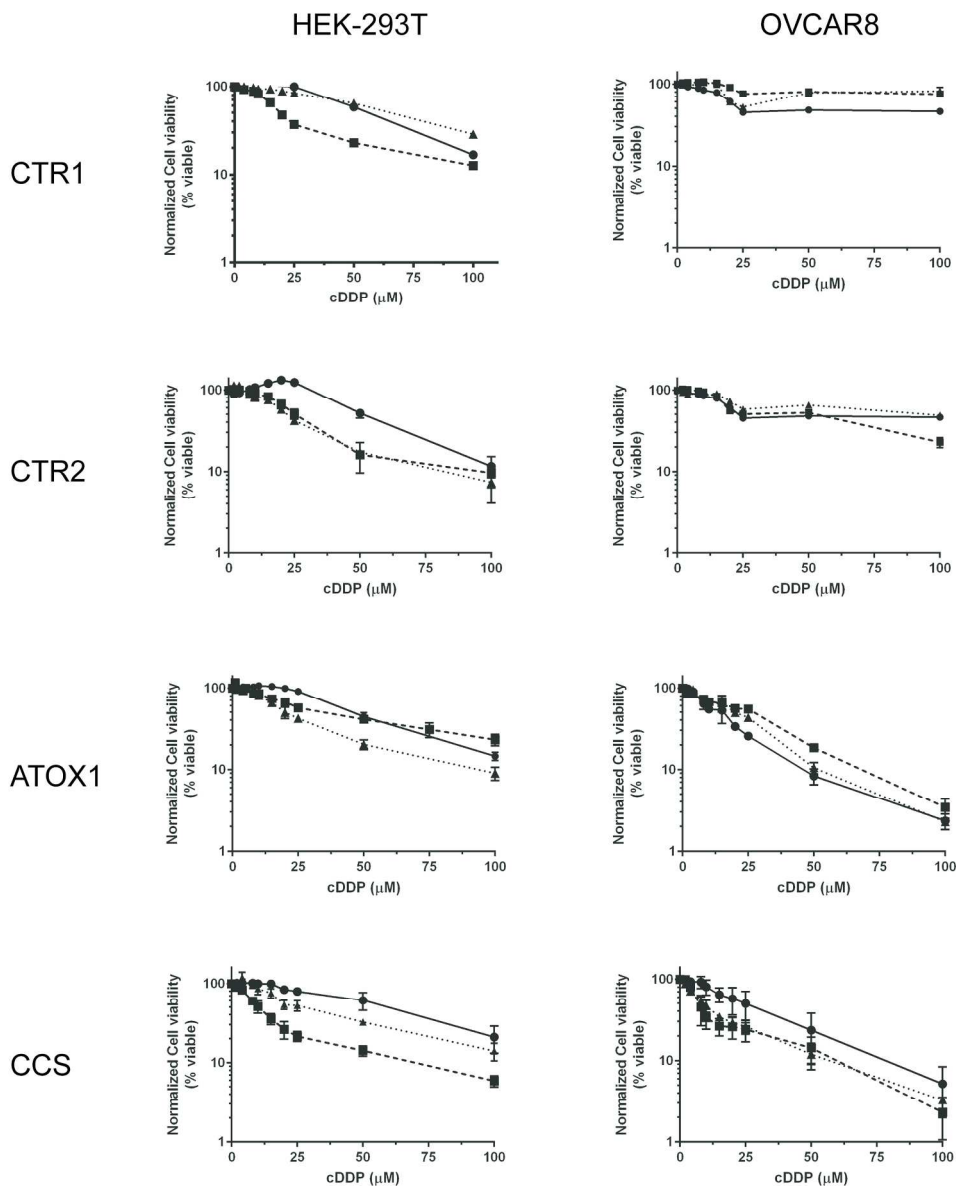


Figure 2. cDDP concentration-survival curves for the wild type HEK-293T and OVCAR8 cell lines and each of the knockout clones. Cells were seeded in 96 well plates and treated with 0-100 μM cDDP for 1 h and then incubated in drug-free medium for an additional 4 days. The data represent the mean \pm SEM of three independent experiments plated in sextuplicate for each drug concentration. For all cell lines circles (\bullet , solid line) represent WT, squares represent KO1 (\blacksquare , dashed line), and triangles (Δ , dotted line) represent KO2.
206x248mm (300 x 300 DPI)

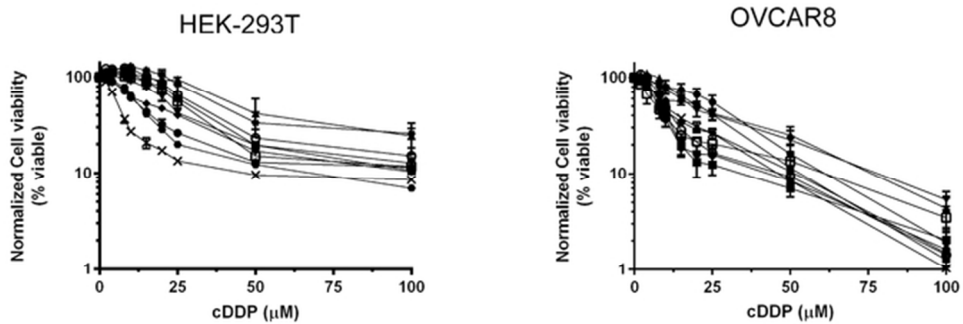


Figure 3. cDDP concentration-survival curves for ten wild type HEK-293T or OVCAR8 subclones. Ten subclones were sorted from the parental population. Cells were seeded in 96 well plates and treated with 0-100 μM cDDP for 1 h and then incubated in drug-free medium for an additional 4 days. The data represent the mean ± SEM of two independent experiments plated in sextuplicate for each drug concentration.
59x20mm (300 x 300 DPI)

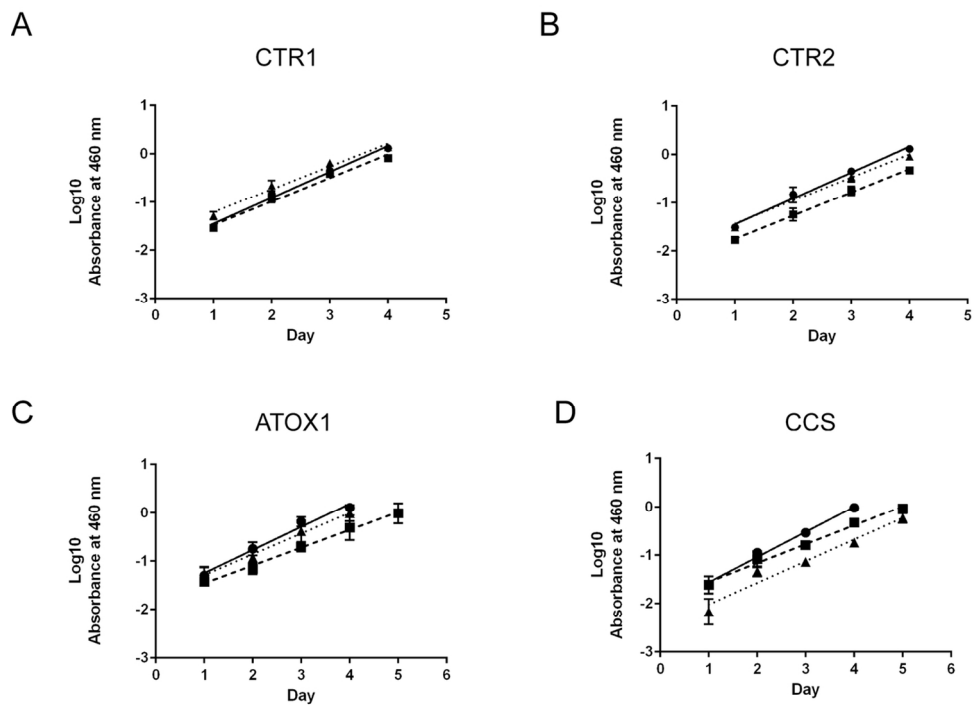


Figure 4. Growth rates of the parental HEK-293T and knockout cells in culture. A) CTR1, B) CTR2, C) ATOX1, and D) CCS. Cells were seeded in 96 well plates and cell viability was quantified every 24 hours. The data were log₁₀ transformed and the linear data for cell growth were fit with a linear trend line shown. All data represent the mean \pm SEM of three independent experiments plated in quadruplicate. For all cell lines circles (●, solid line) represent WT, squares represent KO1 (■, dashed line), and triangles (△, dotted line) represent KO2.

123x89mm (300 x 300 DPI)

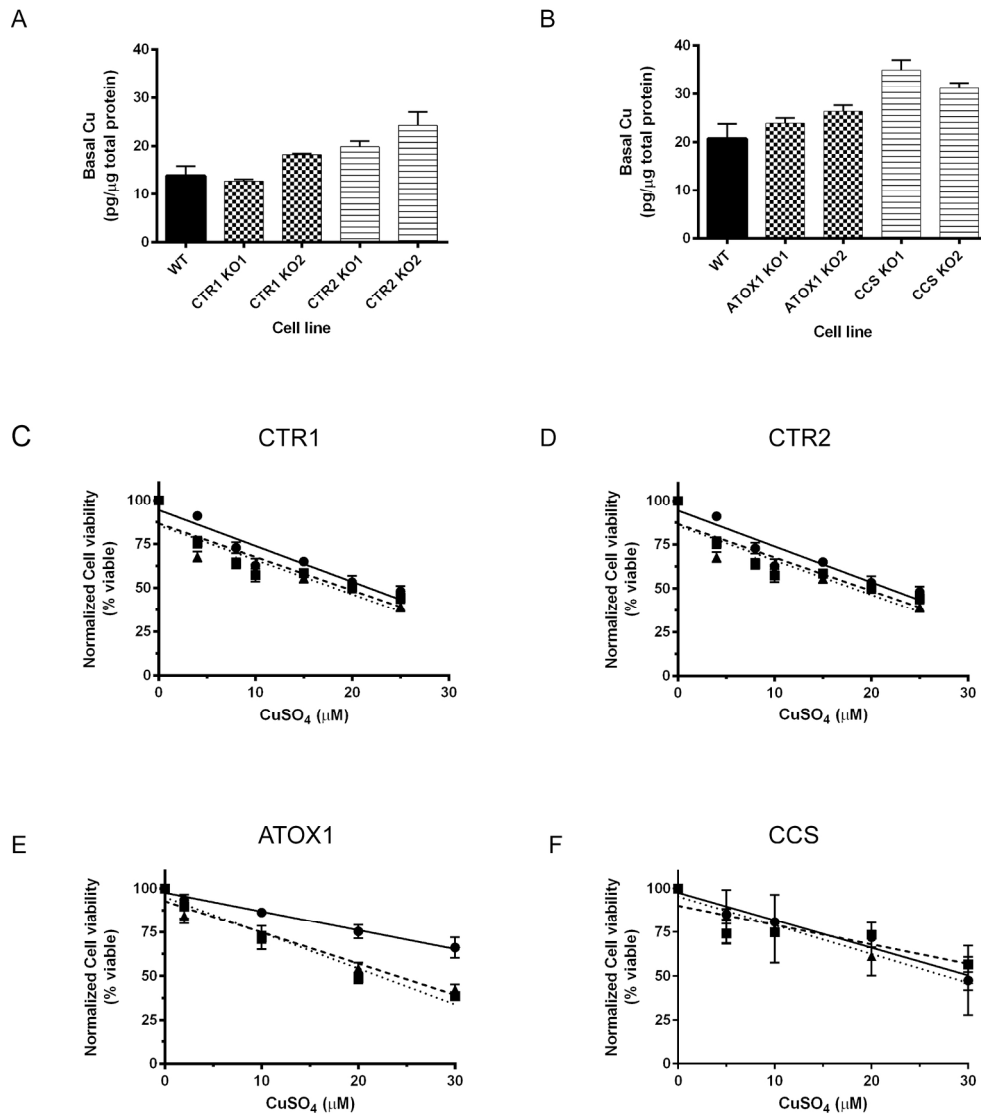


Figure 5. Copper homeostasis in HEK-293T parental and knockout cell lines. A, B) Basal whole cell Cu concentrations in the wild-type (WT) and all knockout (KO) cell lines. P-value WT vs.: CTR1 KO1 = 0.62; CTR1 KO2 = 0.09; CTR2 KO1 = 0.06; CTR2 KO2 = 0.04. P-value WT vs.: ATOX KO1 = 0.02; ATOX1 KO2 = 0.06; CCS KO1 <0.01; CCS KO2 <0.01. Cells were plated in 6-well plates, and each well was harvested for basal Cu quantification with ICP-MS. Copper concentrations were normalized to the average total protein concentration from a second 6-well plate. The data represent the mean \pm SEM of three independent experiments plated in sextuplicate. C-F) Cu sensitivity stress test in the C) 293T CTR1 knockout cell lines, D) 293T CTR2 KO cell lines, E) 293T ATOX1 KO cell lines, and F) 293T CCS KO cell lines. For all cell lines circles (\bullet , solid line) represent WT, squares represent KO1 (\blacksquare , dashed line), and triangles (\blacktriangle , dotted line) represent KO2. Cells were plated in 96 well plates in media supplemented with 0-30 μ M CuSO₄ and incubation in culture for 4 days. The data represent the mean \pm SEM for three independent experiments plated in triplicate.

193x221mm (300 x 300 DPI)

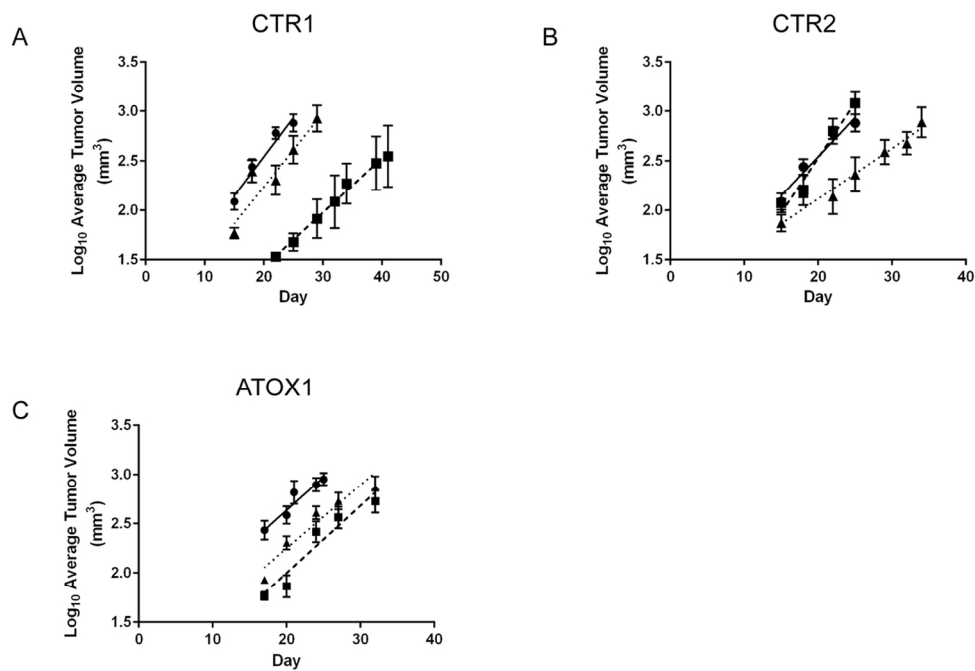


Figure 6. HEK-293T wild type and CTR1, CTR2, and ATOX1 knockout tumor growth in nude mice. Six-week old female nu/nu mice were injected with 1×10^6 cells. Tumor growth was measured over a period of 30-50 days and log_{10} transformed. A) CTR1 KOs, B) CTR2 KOs, and C) ATOX1 KOs. For all cell lines circles (\bullet , solid line) represent WT, squares represent KO1 (\blacksquare , dashed line), and triangles (Δ , dotted line) represent KO2. The linear growth rates of the transformed data were calculated and statistically compared among the 293T WT and KO cell lines. N=5-8 tumors CTR1, 8 tumors CTR2, and 15-16 tumors for ATOX1. 117x81mm (300 x 300 DPI)